CRACK GROWTH AROUND STRESS CONCENTRATIONS IN PIPES AND TUBES

K. Loncke[1], W. De Waele[1], J. Van Wittenberghe[1] T. Galle[1] and P. De Baets[1]

[1] Ghent University, Laboratory Soete, Belgium

Abstract Fatigue crack growth behaviour in pipes fundamentally differs from fatigue growth in shafts and flat plates. The aim of this paper is to give a better understanding of this phenomenon. In a first part of the paper, the general principles of the fracture mechanics are concisely described. The energy approach as well as the stress intensity factor (SIF) approach are explained. An analytical method, a numeric method as well as an experimental method to determine the SIF are discussed. Special attention is given to the experimental method. A theoretical model predicting the deflection of a pipe tested in a resonant bending test setup is evaluated and compared to experimental measured deflections. Several methods to measure the crack growth in a pipe during and after a fatigue bending test are discussed. In addition, an overview is given of results obtained by other authors in the field of fatigue crack growth behaviour of pipes.

Keywords: pipes, stress intensity factor, resonant bending fatigue, fatigue crack growth, crack growth measurement

1 INTRODUCTION

Pipes and tubes are used in many constructions such as e.g. wind farms, offshore platforms and pipelines. Some of those constructions suffer from premature failure due to fatigue cracking, which is likely to occur around stress concentrations. It is therefore important to have a good understanding of the fatigue cracking behaviour around those stress concentrations.

As a first part of this paper, general principles of fracture mechanics are briefly introduced. Subsequently, analytical, numerical and experimental methods to determine the stress intensity factor are discussed. A closer look is taken at a resonant bending fatigue test rig available at Laboratory Soete and possible methods to determine crack initiation and growth when conducting a test. Finally, experimental results obtained by several authors are discussed.

2 DETERMINATION OF STRESS INTENSITY FACTOR

2.1 Fracture mechanics concepts

The fundamental theorem of the energy approach states that crack growth can only occur when there is sufficient energy to encounter the crack growth resistance of the material. The energy release rate J, which is a measure of the energy available for an increment of crack extension, can be expressed as a contour integral [1]. Consider an arbitrary counter clockwise path (Γ) around the crack tip, as illustrated in Figure 1. The J contour integral is given by:

$$J = \int_{\Gamma} \left(w.dy - T_i \frac{\partial u_i}{\partial x} ds \right)$$
(1)

Where w is the strain energy density, T_i are components of the traction vector, which is a stress vector normal to the contour, u_i are the displacement vector components and ds is a length increment along the contour Γ.
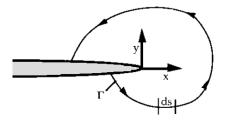

Figure 1. Arbitrary contour around crack tip [1]

The theory of linear elastic fracture mechanics (LEFM), applicable to high cycle fatigue, can be formulated using the stress intensity factors (SIF) K_I, K_{II} and K_{III}, depending on the loading mode (see Figure 2).
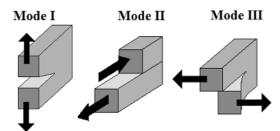

Figure 2. The three loading modes considered in LEFM

When only considering a mode I load, the stresses in the proximity of a crack tip can be calculated using equation 4, where a polar coordinate system (r, θ) with origin at the crack tip is used [2]:

$$\sigma_{xx} = \frac{K_I}{\sqrt{2\pi r}}.\cos\frac{\theta}{2}\left(1-\sin\frac{\theta}{2}\sin\frac{3\theta}{2}\right)$$

$$\sigma_{yy} = \frac{K_I}{\sqrt{2\pi r}}\cos\frac{\theta}{2}\left(1+\sin\frac{\theta}{2}\sin\frac{3\theta}{2}\right) \qquad (2)$$

$$\tau_{xy} = \frac{K_I}{\sqrt{2\pi r}}\sin\frac{\theta}{2}\cos\frac{\theta}{2}\cos\frac{3\theta}{2}$$

The stress intensity factor is related to the J integral as follows:

$$J = \frac{K_I^2}{E} \qquad (3)$$

Where E is the Young's modulus of the material.

The rate of crack growth da/dn can be calculated using the well known Paris law:

$$\frac{da}{dn} = C.\Delta K_I{}^m \qquad (4)$$

Where C and m are material constants. Alternatively, more advanced crack growth equations can be used [3].

2.2   Analytical determination

Analytical formulas to determine K_I are available for a limited number of loading conditions and geometries. The main focus of this work is on semi-elliptical external surface flaws in pipes loaded with a bending moment. For such a case, the analytical formula is as follows [4]:

$$K_I = \sqrt{\pi a}.\sigma_{bg} f_{bg}\left(\frac{a}{t},\frac{a}{2c},\frac{t}{r_i}\right) \qquad (5)$$

where a, t, c and r_i are geometrical parameters, illustrated in Figure 3. The bending load is quantified by the global bending stress σ_{bg} at the outer fibre of the pipe. The factor f_{bg} can be found in tabulated form [4]. However, numerical values of this factor are only available for a limited range of geometrical parameters.
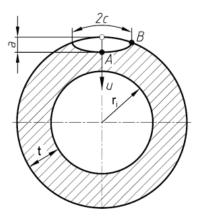
Figure 3. Geometrical parameters for a semi-elliptical surface flaw in a pipe [4]

2.3 Numerical determination

To overcome the limitations of the analytical method, use can be made of a numerical determination of the SIF. There are several ways in which this can be achieved.

A first approach is by using a solution of the stress field in the proximity of the crack tip. The SIF can then be calculated using equation 6, which is based on equation 2 [5]:

$$K_I = \frac{\sqrt{2\pi}}{\cos\dfrac{\theta}{2}\left(1 - \sin\dfrac{\theta}{2}\sin\dfrac{3\theta}{2}\right)} \lim_{r \to 0} \sigma_{xx}\sqrt{r} \tag{6}$$

Similar formulas can be obtained based on σ_{yy} and τ_{xy}. However, the need for an accurate solution for the stress components in the proximity of the crack tip imposes major limitations to this method.

A second approach is based on energy considerations, using the contour integral for the energy release rate J, as given in equation 3. There is no need for an accurate solution in the proximity of the crack tip. This is a main advantage of this method, encouraging its use.

A third and last numerical method makes use of a weight function. Rice [6] showed that two solutions for K_I for the same geometry but different loadings, $K_I^{(1)}$ and $K_I^{(2)}$, are related by:

$$K_I^{(2)} = \frac{E}{2K_I^{(1)}}\left[\int_\Gamma T_i \frac{\partial u_i^{(1)}}{\partial a} d\Gamma + \int_A F_i \frac{\partial u_i^{(1)}}{\partial a} dA\right] \tag{7}$$

As $K_I^{(1)}$ and $K_I^{(2)}$ are arbitrarily chosen, $K_I^{(1)}$ can also be written as:

$$K_I^{(1)} = \int_S \sigma(x).m(x,a)dx \tag{8}$$

Where m(x,a) is a weight function. This weight function method is especially useful in the context of parametric studies. Since a parametric study is not the purpose of this work, the method based on the energy release rate J is preferred.

2.4 Experimental determination

A disadvantage of both the analytical and the numerical methods for determination K_I is that the results do not necessarily represent the real situation. Therefore experiments are still required to verify the results obtained by these methods.

The SIF can be obtained by measuring the crack growth when applying cyclic loads. The gathered data can be substituted in the Paris law (eq. 3) to determine the SIF. This method presumes the material constants C and m are known.

For the execution of this method it is required to apply a well controlled load as well as to measure accurately the crack growth. Both issues are discussed in the remainder of this paper.

3   RESONANT BENDING OF A PIPE

To study the fatigue behaviour of a pipe, cyclic loading will be applied, using a resonant bending fatigue setup available at laboratory Soete (see Figure 4). This setup imposes a load on a pipe by subjecting it to a dynamic excitation with a frequency close to its natural frequency. This causes the pipe to come into resonance, which means that the pipe will deform according to a standing wave that rotates at the excitation frequency.

A theoretical model to calculate the eigenfrequencies, eigenmodes and the deflection of the pipe at an applied excitation frequency, named the 'Free Floating Pipe' model, is developed in [7]. A first test series was conducted to verify the theoretical model for different excitation frequencies. The steel pipe has a diameter of 323,9 mm, a wall thickness of 12,7 mm and a length of 4,82 m. The eigenfrequency of the pipe was calculated to be 34,87 Hz.

The excitation force is exerted by an eccentric mass, rotating at one of the pipe's ends with different excitation speeds. Six different excitation speeds were applied. This resulted in a maximum bending stress ranging from 55 MPa to 169 MPa, for the lowest and highest applied excitation frequency respectively. The deflection of the pipe was measured using the photogrammetric system Pontos, making images of markers glued on the vibrating pipe, at a rate of 500Hz. The measurement with the Pontos system resulted in graphical as well as numerical data about the pipe's deflection. The numerical data was processed and the deflection of the pipe at the six different excitation speeds was compared to the calculated deflection according to the theoretical model. As can be seen in Figure 5, the calculated and measured deflections agreed well.
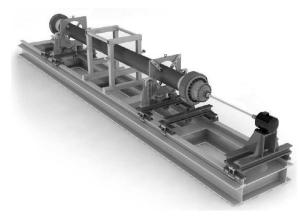

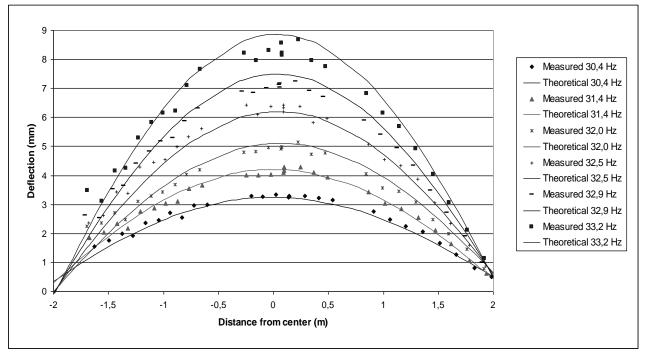Figure 4. Resonant bending fatigue setup [7]

Figure 5. Comparison between the theoretical deflection and the measured deflection at different excitation frequencies

In comparison with the measured deflections, the theoretical model does predict a higher amplitude at frequencies close to the first eigenfrequency. This can be explained by the fact that the theoretical model does not take into account the damping of the pipe.

At the highest excitation frequency, an increase in noise on the measurements can be seen. Its cause will be investigated in future work.

The comparison between the theoretical deflection and the measured deflection learns that the theoretical model can give a good prediction of the deflection of the pipe, as long as the excitation frequency sufficiently differs from the first eigenfrequency of the pipe.

4   RESULTS FROM LITERATURE

Several authors already studied crack growth behaviour of pipes. It is general practice to assume that a realistic part-through crack a in thick-walled pipe can be modelled by a semi-elliptical shaped crack [8].

4.1   Numerical results

A. Carpinteri et al. [8-11] performed finite element simulations of pipes with a semi-elliptical shaped crack under various loading cases. By studying the SIFs along the crack front, it was concluded that the maximum SIF can either be located at the deepest point or at the surface points of the crack. This depends on the dimensions of the crack relative to the pipe dimensions. Those relative dimensions are expressed through a number of dimensionless numbers:

$$\xi = \frac{a}{t}, \qquad \alpha = \frac{a_{el}}{b_{el}}, \qquad s = \frac{a_{el}}{a} \qquad (10)$$

respectively the relative crack depth, the crack aspect ratio and the ellipse shift ratio. The meaning of a, a_{el}, b_{el} and t can be seen in Figure 8.
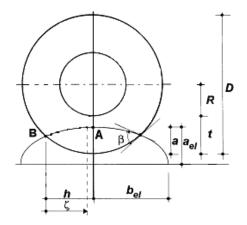

Figure 8. Dimensions of crack and pipe [11]

When the crack aspect ratio α is higher than a certain transition ratio α_t, the highest SIF along the crack front is located at the surface points (Point B in Figure 8). When the crack aspect ratio α is lower than α_t, the maximum SIF will be found at the deepest point of the crack (Point A in Figure 8). The value of α_t depends on the relative crack depth ξ, the relative wall thickness of the pipe R/t and the ellipse shift ratio s.

With regard to pipes loaded by rotational bending, Carpinteri et al. found a value for the transition ratio α_t of 0,8 in case of a relative crack depth ξ=0,2, an ellipse shift factor s=1 and relative wall thickness R/t=1, indicating a thick-walled pipe. When the relative crack depth was ξ=0,8 and the values for the ellipse shift factor and the relative wall thickness were unchanged, a value of 0,6 for α_t was found.

In addition, their finite element simulations showed that the centre of the ellipse tends to shift towards the external circumference during crack growth for an initial ellipse shift factor greater than one [11].
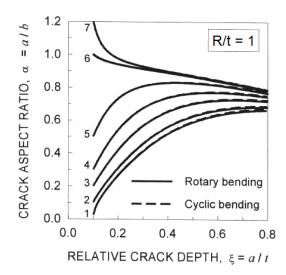
Figure 9. Comparison of growth paths during rotary and cyclic bending [9]

Carpinteri et al. also studied the crack growth during rotary bending and compared their results with those obtained for cyclic bending. Within the range of crack dimensions studied for pipes with a relative wall thickness R/t=1, the crack growth paths of both loading cases seemed to be almost coincident (See Figure 9).

4.2 Experimental results

Singh et al. [12] performed four point bending experiments on pipes with diameter of 219mm and wall thickness of about 15,1 mm. The dimensions of the notches, according to Figure 3, and the applied loads can be found in Table 1. The notches cover a significantly large part of the pipes' circumference. Remarkably, no crack growth in the circumferential direction was noticed during the performed four point bending fatigue test, as long as the crack did not propagate through the wall thickness of the pipe.

Table 1. Dimensions of the notches and the applied loads by P.K. Singh et al. [12]

D_o (mm)	t (mm)	2c (mm)	a (mm)	Load (kN)	R	2c/a	a/t	$2c/(D_o\pi)$	grow through wall
219	15,58	114,3	2,01	200	0,1	56,87	0,13	0,17	273000
219	15,38	113,4	1,97	250	0,5/0,3	57,56	0,13	0,16	869000
219	15,12	110	3	200	0,5	36,67	0,20	0,16	572000
219	15,38	113	3,5	160	0,1	32,29	0,23	0,16	104000
219	15,17	113,8	5,98	200	0,5	19,03	0,39	0,17	252000
219	15,13	113,2	5,5	160	0,1	20,58	0,36	0,16	---

In a previous study, a pipe was tested, using the resonant bending fatigue setup at Labo Soete [7]. The dimensions of pipe and notches, together with the applied load amplitude can be found in Table 2. In this test, circumferential crack growth was noticed before the height of the crack reached the wall thickness. More detailed investigation is necessary to characterise the direction of crack growth and the corresponding shape of the crack front in detail.

Table 2. Dimensions of pipe and notches together with the applied loads by Labo Soete

D_o (mm)	t (mm)	2c (mm)	a (mm)	Stress amplitude (Mpa)	R	2c/a	a/t	$2c/(D_o\pi)$
323,9	23,9	37	7	83,3	-1	5,29	0,29	0,036
323,9	23,9	45	8	66,5	-1	5,63	0,33	0,046
323,9	23,9	39	8	71,7	-1	4,88	0,33	0,041

When comparing the results obtained by Singh et al. and laboratory Soete, it must be noticed that a wide initial crack will grow less in the circumferential direction as compared to a narrow crack. However there are several differences to the other crack dimensions and applied load. The notches used at laboratory Soete

have shorter lengths and a rotating load, were as Singh et al. use long notches with a cyclic load. This makes it rather difficult to make a good comparison.

5   DETERMINING CRACK INITIATION AND GROWTH

When conducting fatigue tests on a pipe, not only a well controlled load must be applied, the crack initiation and growth should also be accurately determined. There are several methods available, each with their own limitations. The most established methods for crack detection and sizing are visual inspection, dye penetrant inspection, magnetic particle inspection, leak tests, ultrasonic inspection and radiographic inspection [7,13-18]. As the principles of these methods are considered to be well known, the focus will be on some possibly less common methods.

5.1   Beach marking

The beach marking method is executed during the propagation stage of a fatigue test. During the fatigue test, the maximum applied load is kept constant. At a number of predefined moments during the propagation stage, the minimum applied load is changed. This changes the K_I, and according to the Paris law (eq. 3), this causes changes in the crack growth rate. After the fatigue test and a subsequent brittle fracture of the remaining uncracked material, those changes in crack growth rate can be seen as differences in the surface roughness, the so-called beachmarks. Lines on the crack surface will represent the different crack fronts during the propagation phase (See Figure 6), and allow to quantify crack growth rates. [19]
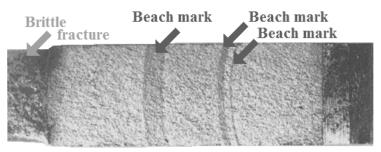

Figure 6. Fracture surface with beach marks [19]

5.2   Crack opening displacement

By measuring the transverse crack opening during a fatigue test, it becomes possible to estimate the depth of the crack through a correlation method [20, 21]. The transverse crack opening can be measured using a clip gage or LDVT. The need for knowledge of the correlation between transverse crack opening and crack depth, imposes a major restriction on this method. With regard to the resonant bending fatigue setup, the use of a clip gage or LDVT is rather difficult because of the large accelerations of the pipe.

5.3   Eddy current testing

In the execution of this method, a primary magnetic field is applied to the material by the use of a coil. This causes eddy currents in the material, which in turn are causing a secondary magnetic field. Cracks in the material will disturb the eddy currents and the secondary magnetic field. Thus by measuring changes in the secondary magnetic field, cracks can be detected [22]. The method is rather suited for crack detection then for crack sizing. With this technique it is possible to not only detect surface flaws, but also internal defects within a limited distance of the surface.

5.4   Alternating current field measurement (ACFM)

A similar method is the alternating current field measurement. Again eddy currents are generated by a coil. Instead of measuring the secondary field, whit this method the potential differences over a surface are measured. When a crack is present, this will result in a larger potential drop, making detection of cracks possible. Cracks with depths of less then 1 mm can be detected, with an accuracy of 0,3 mm [23].

5.5   Electrical resistance based methods (DCPD/ACPD)

With this method, a direct (DCPD) or alternating (ACDP) electrical current is injected in the material. When an internal crack or a surface crack is present, the electrical resistance around the crack is increased, causing a greater potential drop.

When using the ACPD method, an additional effect takes places: the 'skin-effect' [24]. This effect will cause the current to flow within a thin layer adjacent to the surface. The thickness of the thin current layer can be

adjusted by changing the frequency of the current. Since the current only flows close to the surface, a surface crack will cause a larger potential drop, compared to the DCPD method. This technique allows for crack sizing, but is less suited for crack detection.

5.6 Thermographic measurements

This technique is based on the measurements of temperature differences around defects at the surface of a component, using an infrared camera. There are several ways to cause temperature differences around cracks.

A first method is vibrothermography [25] in which the component is subjected to mechanical vibration. Those vibrations will cause heat generation at defects through friction.

It is also possible to create temperature differences by inductive heating [26-29]. A coil with an alternating current is brought into the proximity of the component's surface. The alternating current causes eddy currents within the material. Due to the higher electric resistance around cracks, the material will heat up in the proximity of a crack. This is illustrated in Figure 7.
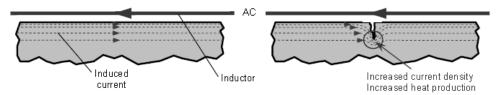

Figure 7. Principles of inductive thermography [29]

A last way to create temperature differences is through cyclic deformation of the component [30, 31]. From the energy necessary for deformation of a component during a fatigue test, only 5 to 10% is used for irreversible structural changes within the material. The remaining part is dissipated as heat.

When a fatigue test is performed with a low frequency, the dissipated power is low and consequently the temperature differences are also low. Medgenberg and Ummenhofer [30] have performed fatigue tests under axial tension with a frequency of 15 Hz, while measuring the temperature differences over the tested component. The temperature difference they measured was rather small, about 15 mK. In the resonant bending setup, the excitation frequency may be up to 40Hz. At those frequencies there is a higher heat generation is expected. It might be clear that accurate measurement equipment is needed.

5.7 Analysis of stiffness changes

When a crack is present in a component, this leads to a decrease in its stiffness. This results in a decrease of the eigenfrequenties of the component, as well as in an increase of the deflection corresponding to a certain predefined load. The changes in eigenfrequencies can be measured using accelerometers and dynamic strain gauges after excitation of the pipe with an impact [32]. An increase of the deflection of the pipe can be measured, using a photogrammetric system, like the Pontos system [33]. Inverse methods can be used to correlate the output to stiffness change and crack depth.

6 CONCLUSIONS

In this paper, analytical, numerical and experimental methods for determination of K_I for a semi-elliptical surface notch in a pipe subjected to bending is discussed. The resonant bending fatigue setup available at Laboratory Soete is briefly discussed. A satisfactory agreement between the theoretical model describing the deflection of the pipe during bending and the measured deflection is found. When the excitation frequency comes into the proximity of the resonance frequency of the pipe, the accuracy of the theoretical model is reduced, due to not taking into account the damping of the pipe. Several methods to determine crack initiation and growth during a fatigue test are discussed. Finally an overview of numerical and experimental results related to the fatigue behaviour of pipes, obtained by other authors, is given.

With respect to the continuation of this research, a pipe will be tested using the resonant bending fatigue setup. Different notches will be applied to the pipe. It is also intended to numerically determine the SIFs along the crack front. During the fatigue test the beach marking method will be used to measure the crack growth. A challenge is to execute a resistance based measuring method, to give online information during the fatigue test.

7 NOMENCLATURE

a	crack depth	m
A	crack area/ crack surface	m²
C	material constant	-
C_p	heat capacity at constant pressure	J/(kg.K)
E	Young's modulus	GPa
F	work done by external forces	J
F_i	body force	N/m³
J	energy release rate	J/m²
k	thermal conductivity	W/(m.K)
K_i	stress intensity factor	$\mathrm{MPa}\sqrt{\mathrm{m}}$
m	material constant	-
s	ellipse shift factor	-
T	temperature	K
T_i	components of stress vector on the contour *Γ*	N/m²
T_0	reference temperature	K
u_i	displacement vector	m
U	elastic energy	J
w	strain energy density	J/m³
W	energy necessary for crack growth	J
α	*crack aspect ratio*	-
$α_t$	*crack aspect transition ratio*	-
$α_T$	coefficient of thermal expansion	-
Γ	arbitrary contour	-
$ε_{ii}$	elastic strain tensor	-
$\underline{ε}_p$	plastic strain tensor	-
v	Poisson's ratio	-
ξ	relative crack depth	-
ρ	mass density	kg/m³
σ	stress	MPa
$\underline{σ}$	stress tensor	MPa
$σ_{bg}$	maximum outer fibre bending stress	MPa
$σ_y$	stress distribution perpendicular to the crack front	MPa

8 ACKNOWLEDGEMENTS

9   REFERENCES

[1] T.L. Anderson, Fracture mechanism, Fundamentals and applications, Second Edition, CRC Pres, 0-8493-4260-0, 1995

[2] G.R. Irwin, Analysis of stresses and strains near the end of a crack traversing a plate, Journal of applied Mechanics, 61, 361-364, 1957, as referred in [1]

[3] N. Pugno, M. Ciavarella, P. Cornetti, A. Carpinteri, A generalized Paris' law for fatigue crack growth, Journal of the Mechanics and Physics of Solids, 53, 1333-1349, 2006

[4] Fitnet MK7, Annex A: *Stress intensity factor (SIF) solutions,* 2006

[5] T. Joye, J. Pauwels, Stress intensity factor for a surface crack at the thread root of a pipe joint, master thesis, Katholieke Universiteit Leuven, 2008

[6] J.R. Rice, Some Remarks on Elastic Crack-Tip Stress Fields, International Journal of Solids and Structures, 8, 751-758, 1972

[7] J. Van Wittenberghe, Experimental Analysis and Modelling of the Fatigue Behaviour of Threaded Pipe Connections, PhD dissertation, Ghent University, 2011

[8] A. Carpinteri, R. Brighenti, A. Spagnoli, Part-through cracks in pipes under cyclic bending, Nuclear Engineering and Design, 185, 1-10, 1998

[9] A. Carpinteri, R. Brighenti, A. Spagnoli, Fatigue growth simulation of part-through flaws in thick-walled pipes under rotary bending, International Journal of Fatigue, 22, 1-9, 2000

[10] A. Carpinteri, R. Brighenti, Circumferential surface flaws in pipes under cyclic axial loading, Engineering Fracture Mechanics, 60 (4), 383-396, 1998

[11] A. Carpinteri, R. Brighenti, A three-parameter model for fatigue behaviour of circumferential surface flaws in pipes, International Journal of Mechanical Sciences, 42, 1255-1269, 2000

[12] P.K. Singh, K.K. Vaze, V. Bhasin, H.S. Kushwaha, P.Gandhi, D.S. Ramchandra Murthy, Crack initiation and growth behaviour of circumferentially cracked pipes under cyclic and monotonic loading, Pressure Vessels and Piping, 80, 626-640, 2003

[13] Colin G. Drury, Jean Watson, Human Factors Good Practices in Fluorescent Penetrant Inspection, https://hfskyway.faa.gov/HFTest/Bibliography%20of%20Publications/MX%20FAA%28Former%20HFSkyway%29/Other%20Research%20Program%20Reports/1999%20Reports%20Human%20Factors%20Good%20Practices.pdf, December 2011

[14] http://www.ndt.net, December 2011

[15] J.L. Rose, Elements of a Feature-based Ultrasonic Inspection System, Materials Evaluation, 42 (2), 210-218, 1982

[16] S. Dong-Man, K. Whan-Woo, C. Jin-Gyun, Ultrasonic Inspection of Studs (Bolts) Using Dynamic Predictive Deconvolution and Wave Shaping, IEEE Transactions on Ultrasonics, Ferroelectrics, and Frequency Control, 46 (2), 457-463, 1999

[17] http://www.ndt-ed.org/EducationResources/CommunityCollege/Ultrasonics/Introduction/description.htm, December 2011

[18] J. Schors, K.-W. Harbich, M. P. Hentschel, A. Lange, Non-Destructive Micro Crack Detection in Modern Materials, ECNDT, 2006

[19] C. Ragazzo, R.W. Hertzberg, R. Jaccard, A Method for Generating Fatigue Marker Bands Using a Constant Krnax Test Procedure, Journal of Testing and evaluation, 23 (l), 19-26, 1995

[20] S. Nervi, B.A. Szabo, On the estimation of residual stresses by the crack compliance method, Computer Methods in Applied Mechanics and Engineering, 196, 3577–3584, 2007

[21] C.Q. Cai, C.S. Shin, A normalized area-compliance method for monitoring surface crack development in a cylindrical rod, International Journal of Fatigue, 27, 801-809, 2005

[22] T. Chady, M. Enokizono, Crack Detection and Recognition Using an Eddy Current Differential Probe, IEEE Transactions on Magnetics, 35 (3), 1849-1852, 1999

[23] J. Zhou, M.C. Lugg, R. Collins, A non-uniform model for alternating current field measurement of fatigue cracks in metals, International Journal of Applied Electromagnetics and Mechanics, 10, 221-235, 1999

[24] M.C. Lugg, An Introduction to ACPD, Technical Software Consultants Ltd., 2002

[25] X. Maldague, Applications of Infrared Thermography in Nondestructive Evaluation

[26] G. Zenzinger, J. Bamberg, W. Satzger, V. Car, Thermographic Crack Detection by Eddy Current Excitation, http://www.impulsthermografie.com/downloads/Thermographic_Crack_Detection_by__Eddy _Current_Excitation__.pdf, December 2011

[27] G. Walle, U. Netzelmann, Thermographic Crack Detection in Ferritic Steel Components Using Inductive Heating, ECNDT, 2006

[28] S. Štarman, V. Matz, Automated System for Crack Detection Using Infrared Thermographic Testing, 17th World Conference on Nondestructive Testing, Shanghai, China, 25-28 Oct 2008

[29] J. Vrana, M. Goldammer, J. Baumann, M. Rothenfusser, W. Arnold, Mechanisms and Models for Crack Detection with Induction Thermography, AIP conference Proceedings, 975, 475-482, 2007

[30] J. Medgenberg, T. Ummenhofer, Assessment of fatigue damage in low-carbon steel using Lock-In-Thermography, QIRT Open Archives, 8th international Conference on Quantitative Infrared Thermography, 2006

[31] T. Ummenhofer, J. Medgenberg, On the use of infrared thermography for the analysis of fatigue damage processes in welded joints, International Journal of Fatigue, 31, 130-137, 2009

[32] T.T. Bui, G. De Roeck, J. Van Wittenberghe, P. De Baets, W. De Waele, Fatigue Damage identification in threaded connection of tubular structures through in-situ modal tests, Sustainable Construction and Design 2011, Labo Soete, 2011

[33] J. Van Wittenberghe, P. De Baets, W. De Waele, T.T. Bui, G. De Roeck, Evaluation of fatigue crack propagation in a threaded pipe connection using an optical dynamic 3D displacement analysis technique, Engineering Failure Analysis, 18, 1115-1121, 2011